Quantum corrections to the Schwarzschild metric from vacuum polarization

Pau Beltrán-Palau[1,*] Adrián del Río[2,†] and José Navarro-Salas[1,‡]

[1]*Departamento de Fisica Teorica and IFIC, Centro Mixto Universidad de Valencia-CSIC.*
Facultad de Fisica, Universidad de Valencia, Burjassot-46100 Valencia, Spain
[2]*Institute for Gravitation and the Cosmos and Physics Department, The Pennsylvania State University,*
University Park, Pennsylvania 16802 USA

We explore static and spherically symmetric solutions of the 4-dimensional semiclassical Einstein's equations using the quantum vacuum polarization of a conformal field as a source. These solutions may be of interest for the study of exotic compact objects (ECOs). The full backreaction problem is addressed by solving the semiclassical Tolman-Oppenheimer-Volkoff (TOV) equations making use of effective equations of state inspired by the trace anomaly and an extra simplifying and reasonable assumption. We combine analytical and numerical techniques to solve the resulting differential equations, both perturbatively and nonperturbatively in $\hbar$. In all cases the solution is similar to the Schwarzschild metric up to the vicinity of the classical horizon $r = 2M$. However, at $r = 2M + \varepsilon$, with $\varepsilon \sim O(\sqrt{\hbar})$, we find a coordinate singularity. In the case of matching with a static star, this leads to an upper bound in the compactness, and sets a constraint on the family of stable ECOs. We also study the corrections that the quantum-vacuum polarization induces on the propagation of waves, and discuss the implications. For the pure vacuum case, we can further extend the solution by using appropriate coordinates until we reach another singular point, where this time a null curvature singularity arises and prevents extending beyond. This picture qualitatively agrees with the results obtained in the effective two-dimensional approach, and reinforces the latter as a reasonable method.

I. INTRODUCTION

Advances in gravitational wave (GW) astronomy to detect and analyze GWs in the last years [1], as well as the recent progress in very long baseline interferometry [2], are opening new avenues to study strong-field gravity and the physics of black holes. In particular, with the advent of large amounts of data from GW and electromagnetic observations in the future, it will become possible to test and to quantify in precise terms the existence of horizons. As a result, there is a growing interest in studying models of dark, compact horizonless astrophysical objects that may mimic very closely the behavior of black holes in the GW data, and in examining different physical mechanisms that could be used to uncover these exotic compact objects (ECOs) with observations [3].

While there exists a large class of different models that manage to simulate black holes, most of them require going beyond the Standard Model of particles and/or general relativity (GR) [4–10]. This is because similar values of BH compactness are required to mimic GW observations, but

stable astrophysical objects with such compactness are forbidden within GR by Buchdahl's theorem and the classical energy conditions. An appealing possibility is to consider quantum effects (while preserving classical gravity as described by conventional GR), as they can potentially avoid the assumptions of this theorem without requiring exotic assumptions. This involves facing the difficulties of the renormalized stress-energy tensor $\langle T_{ab} \rangle$, describing the gravitational vacuum polarization of quantum fields, and also solving the corresponding semiclassical backreaction equations. So far all methods developed to compute $\langle T_{ab} \rangle$ in quantum field theory in curved spacetime, either analytical or numerical, assume a fixed background metric. Even fixing the background, the explicit computation of $\langle T_{ab} \rangle$ is complicated and only a few examples are known, mainly in cosmology [11–13] and for stationary configurations [14–16]. As a consequence, the problem of solving the full semiclassical Einstein's equations is terribly complicated, even approximately. Since the nontrivial $(t - r)$ part of a spherically symmetric metric is two-dimensional, a popular approach in the past has been to consider the analogous problem in effective $1 + 1$ dimensions. A first attempt in this direction is to truncate the theory to the s-wave sector of the matter field and implement dimensional reduction by integrating the angular

*pau.beltran@uv.es
†axd570@psu.edu
‡jnavarro@ific.uv.es

degrees of freedom. One ends up with an effective two-dimensional theory (i.e., a particular dilaton-gravity theory [17]), which, after further simplifying assumptions (near-horizon approximation), has a semiclassical description univocally determined by the two-dimensional trace anomaly $\langle T \rangle = \frac{\hbar}{24\pi} R^{(2)}$ (this is usually referred to as the Polyakov theory approximation [17]). In two-dimensions the trace anomaly is sufficient to fix the quantum stress-energy tensor, which in turn can be used to produce a reasonable approximation for evaluating static quantum corrections to the Schwarzschild geometry in vacuum. The semiclassical solution is similar to the classical Schwarzschild solution until very close to the event horizon, but the near-horizon geometry is replaced by a bouncing surface for the radial coordinate, mimicking the throat of a nonsymmetric wormhole. A curvature singularity is found beyond the throat [18]. This picture has been confirmed with more analytical details in [19] and also in [20] (using a natural deformation of the Polyakov theory approximation), and very interesting extensions for stellar configurations have been analyzed in [21–23].

The above two-dimensional effective method is expected to provide important insights, but since the problem is very relevant and it is not entirely clear to what extent the two-dimensional approach is really a good approximation, an intrinsic four-dimensional approach is demanded. This is one of the aims of this work. Our strategy here will be to solve the full semiclassical Einstein's equations but without explicitly calculating $\langle T_{ab} \rangle$. Instead, we shall approach the problem as in classical general relativity, by simply giving equations of state and some appropriate boundary conditions. One of the equations of state will be determined by the four-dimensional trace anomaly, which is independent of the choice of quantum state. More specifically, we will consider a conformal quantum field, in which the trace of $\langle T_{ab} \rangle$ is entirely determined by the anomaly. Then, we will assume a natural condition on the tangential pressure which we expect to capture the main qualitative aspects of the actual solution (we differ here from the assumptions given in [24]). This will make the problem manageable and will allow us to approach the problem directly in four dimensions.

In this new framework we will also be interested in investigating whether there exists physically reasonable, horizonless "vacuum" geometries which may mimic black holes (e.g., wormholes), as well as analyzing what implications the quantum vacuum-polarization from the exterior geometry may have on static ECOs. Uniqueness theorems in classical GR tell us that the exterior vacuum solution of any ECO must be described by the Schwarzschild metric, and this is widely taken for granted in the literature. However, quantum fields exist all around, and their presence may break this degeneracy with respect to black holes.

Even though semiclassical gravity may provide a conservative framework for studying the formation and/or exterior geometry of exotic astrophysical objects,

for solar-mass scales it is often expected that quantum effects should only lead to extremely low corrections of the classical solutions, in such a way that from an observational point of view the difference is totally negligible. Remarkably, recent works developed by different independent groups have shown that even tiny corrections to the metric may significantly alter the quasinormal mode (QNM) frequency spectrum of black holes [25–28], opening the possibility of constraining these quantum corrections with GW spectroscopy. Incidentally, this provides a fantastic opportunity to test quantum field theory in astrophysics and adds further motivation to address the historical difficulties encountered when solving the semiclassical Einstein's equations.

The paper is organized as follows. In Sec. II we provide the setup of the calculation by writing down the central equations, as well as by specifying and motivating the assumptions in our problem. Then in Sec. III we solve the differential equations, combining both analytical and numerical techniques, and highlight the main features of the solution obtained, as well as the implications for ECOs. In Sec. IV we obtain the maximal extension and describe the curvature singularity that arises. Section V is devoted to physical applications of the obtained semiclassical metric. In particular we derive the dynamical equations governing scalar and electromagnetic waves, estimate the associated light-ring frequencies using the WKB approximation, and compare them with the Schwarzschild case. Finally, in Sec. VI we present our conclusions.

Our conventions are as follows. We work in geometrized units $G = c = 1$ and keep $\hbar$ explicit throughout. The metric signature has signature $(-, +, +, +)$, ∇_a will denote the associated Levi-Civita connection, the Riemann tensor is defined by $2\nabla_{[a}\nabla_{b]}v_c =: R_{abc}{}^d v_d$ for any 1-form v_d; the Ricci tensor is defined by $R_{ab} := R_{acb}{}^c$; and the scalar curvature is $R := g^{ab}R_{ab}$. All tensors and functions are assumed to be smooth, unless otherwise stated.

II. SEMICLASSICAL TOV EQUATIONS IN QUANTUM VACUUM

Our aim in this work is to study solutions of the semiclassical Einstein's equations

$$G_{ab} = 8\pi(\langle T_{ab} \rangle + T_{ab}^{\text{classical}}), \qquad (1)$$

in order to find an effective metric that may describe quantum corrections to classical black hole spacetimes induced by the quantum vacuum, or even a new family of solutions. Here $T_{ab}^{\text{classical}}$ represents some classical gravitational source, while $\langle T_{ab} \rangle$ denotes the expectation value of the stress-energy tensor, evaluated for some vacuum state $|0\rangle$ of some given quantum field living on the background metric g_{ab} that solves the above equations. For $T_{ab}^{\text{classical}} = 0$ and in the absence of quantum fields the spherically

symmetric solution is a Schwarzschild black hole due to Birkhoff's theorem. But if a quantum field is included, $\langle T_{ab}\rangle \neq 0$, and we expect to get a Schwarzschild-type deformed metric due to quantum vacuum effects ascribed to that field. Solving this problem requires finding a vacuum state $|0\rangle$ and a metric g_{ab} that together solve (1). For reasons that we will discuss in more detail below, this is an extraordinary problem and there are currently no systematic techniques available to address the full question. Our strategy will consist in fixing some desirable properties for the vacuum state and solving the resulting PDE for g_{ab}. More precisely, we will demand the vacuum state to be static and invariant under the group of rotations. This may be thought of as the most immediate quantum generalization of the classical Schwarzschild vacuum. The solution to (1) will then correspond to a spherically symmetric and static metric, which in global coordinates $\{t, r, \theta, \phi\}$ can be written as [29]

$$ds^2 = -e^{-2\phi(r)}dt^2 + \frac{dr^2}{1 - \frac{2m(r)}{r}} + r^2 d\Omega^2. \qquad (2)$$

Physically, the assumption of staticity is fundamental for studying the exterior vacuum region of exotic compact objects (ECOs) that are stable. For black holes, on the other hand, it is well-known that the assumption of staticity leads to the Boulware state, which gives rise to divergences in the stress-energy tensor at the classical horizon [30]. However, this conclusion holds only when the renormalized stress-energy tensor is computed for a test quantum field on a fixed Schwarzschild background. In this work we will evaluate the implications of staticity when considering the whole problem, including the backreaction effect that the quantum vacuum may produce in the metric.

To get the specific values of the metric components in (2) we have to solve (1) for $T_{ab}^{\text{classical}} = 0$. For a static and spherically symmetric vacuum state the most general expression for the renormalized stress-energy tensor $\langle T_{ab}\rangle$ is

$$\langle T_{ab}\rangle = -\langle\rho(r)\rangle u_a u_b + \langle p_r(r)\rangle r_a r_b + \langle p_t(r)\rangle q_{ab}, \qquad (3)$$

where $u_a = e^{-\phi}\nabla_a t$ is a timelike vector normalized as $u^2 = -1$, $r_a = (1 - \frac{2m(r)}{r})^{-1/2}\nabla_a r$ is a unit spacelike vector, and q_{ab} is the metric on the unit 2-sphere. The metric can be written covariantly as $g_{ab} = -u_a u_b + r_a r_b + q_{ab}$. There are only three independent equations from the semiclassical Einstein equations. On the other hand, there is one non-trivial Bianchi identity. Collecting the tt and rr Einstein's equations and this Bianchi identity we get the following equations

$$\frac{dm(r)}{dr} = 4\pi r^2 \langle\rho(r)\rangle, \qquad (4)$$

$$\frac{d\phi(r)}{dr} = -\frac{m(r) + 4\pi r^3\langle p_r(r)\rangle}{r^2(1 - \frac{2m(r)}{r})}, \qquad (5)$$

$$\frac{d\langle p_r(r)\rangle}{dr} = -\frac{m(r) + 4\pi r^3\langle p_r(r)\rangle}{r^2(1 - \frac{2m(r)}{r})}(\langle\rho(r)\rangle + \langle p_r(r)\rangle)$$
$$- \frac{2}{r}(\langle p_r(r)\rangle - \langle p_t(r)\rangle). \qquad (6)$$

When $\langle p_r\rangle \neq \langle p_t\rangle$, there are anisotropic pressures. In the isotropic case this system of equations reduces to the usual Tolman-Oppenheimer-Volkoff (TOV) equations. In the rest of the work we will refer to this system of equations as the semiclassical TOV equations.

In this system there are 5 unknowns (3 from the stress-energy tensor and 2 from the metric) for 3 equations. Normally one would compute $\langle T_{ab}\rangle$ and express the result in terms of $\phi(r)$ and $m(r)$ in order to get the system above solved. Instead, we will impose two functional relations between the components of the stress-energy tensor, in order to avoid such a difficult (or unattainable) calculation. First, we will consider the case of a massless quantum field conformally coupled to the spacetime. The advantage of doing this is that the relation between the three independent components of the stress energy tensor is univocally fixed by the trace anomaly $\langle T_a^a\rangle$ as

$$-\langle\rho\rangle + \langle p_r\rangle + 2\langle p_t\rangle = \langle T_a^a\rangle, \qquad (7)$$

and the trace anomaly is uniquely determined by the geometry of the spacetime

$$\langle T_a^a\rangle = \frac{\hbar}{2880\pi^2}(\alpha C^{abcd}C_{abcd} + \beta R^{ab}R_{ab} + \gamma R^2 + \delta\Box R). \qquad (8)$$

In this expression C_{abcd} is the Weyl tensor, R_{ab} the Ricci tensor, R the Ricci scalar and α, β, γ, δ are real numbers. Most importantly, this result is independent of the choice of the quantum state. The idea of exploiting the trace anomaly goes back to [31]. The constant coefficients depend on the particular field under consideration. It should be noted though that there exits an intrinsic ambiguity in the trace anomaly for the coefficient δ [32]. This ambiguity is related to the choice of the renormalization scheme. The term with $\Box R$ can always be removed by adding a local counterterm in the Lagrangian so, from now on we set $\delta = 0$. This simplifies the problem considerably, since it will avoid derivatives of second and third order of the metric in the field equations.

By evaluating (8) with our metric and using the semi-classical TOV equations written above one can obtain a simplified expression for the trace anomaly in terms of $\langle\rho\rangle$, $\langle p_r\rangle$ and $\langle p_t\rangle$. This leads to the following equation of state

$$-\langle\rho\rangle + \langle p_r\rangle + 2\langle p_t\rangle = \frac{\hbar}{270}\left[\alpha\left(\frac{3m}{4\pi r^3} - \langle\rho\rangle + \langle p_r\rangle - \langle p_t\rangle\right)^2 + 6\beta(\langle\rho\rangle^2 + \langle p_r\rangle^2 + 2\langle p_t\rangle^2) + 6\gamma(-\langle\rho\rangle + \langle p_r\rangle + 2\langle p_t\rangle)^2\right].$$

(9)

For definiteness in this work we restrict to scalar fields, for which the coefficients are $\alpha = \beta = 1$ and $\gamma = -1/3$. For these values the above expression can be further simplified to

$$-\langle\rho\rangle + \langle p_r\rangle + 2\langle p_t\rangle = \frac{\hbar}{180}\left[\frac{m}{\pi r^3}\left(3\frac{m}{\pi r^3} + 8(-\langle\rho\rangle + \langle p_r\rangle - \langle p_t\rangle)\right) + 8\langle\rho\rangle(\langle\rho\rangle - \langle p_r\rangle + 2\langle p_t\rangle) + 8(\langle p_r\rangle - \langle p_t\rangle)^2\right]. \quad (10)$$

We need another restriction to make our system of equations solvable. Unfortunately there are no other universal geometric properties of the stress-energy tensor that may allow us to fix a similar relation between the different components of the stress-energy tensor. To proceed further we need to impose a condition on $\langle T_{ab}\rangle$ based on what we may expect from the quantum state. We will consider here that $\langle p_r\rangle = \langle p_t\rangle$. This simplifying assumption is inspired by the "zero-order" result that one gets when calculating $\langle T_{ab}\rangle$ in a fixed Schwarzschild background when $r \to 2M$, and we expect this near-horizon approximation to capture the qualitative behavior of the actual solution. Indeed, in a Schwarzschild spacetime background the vacuum expectation value $\langle T_{ab}\rangle$ of a conformal scalar field in the static spherically symmetric state behaves, in the vicinity of the horizon, as [30]

$$\langle T^\nu_\mu\rangle \sim -\frac{\hbar}{2\pi^2(1-2M/r)^2}\int_0^\infty \frac{d\omega\,\omega^3}{e^{8\pi M\omega}-1}\begin{bmatrix} -1 & 0 & 0 & 0 \\ 0 & \frac{1}{3} & 0 & 0 \\ 0 & 0 & \frac{1}{3} & 0 \\ 0 & 0 & 0 & \frac{1}{3} \end{bmatrix}.$$

(11)

Both $\langle T^\theta_\theta\rangle \equiv \langle p_t\rangle$ and $\langle p_r\rangle \equiv \langle T^r_r\rangle$ merge for $r \to 2M$, but as one moves away from the vicinity of the horizon, the tangential and radial pressures start to differ. In fact, for $r \to \infty$ one has $\langle p_r\rangle = -\frac{1}{3}\langle p_t\rangle \sim \mathcal{O}(r^{-5})$ [33]. Therefore, our assumption is expected to work only qualitatively as an approximation to the actual relationship, whose knowledge requires computing $\langle T_{ab}\rangle$ in detail. This simplification is expected to capture the main physical ingredients of our field theory (the results obtained will be exact at least in a neighborhood of the classical horizon).

Our approach can be easily compared with other works by fixing this free condition with different assumptions. For instance, the effective two-dimensional Polyakov approximation [18,19,21,22] can be regarded as fixing trivially the tangential pressure $\langle p_t\rangle = 0$ (or with additional extra deformations [20,23]) and restricting the trace anomaly

to its two-dimensional value. Instead, we are trying to solve the 4D problem directly without assuming a priori that it is similar to the 2-dimensional case. On the other hand, the approach of [24] also quantizes the matter field in four dimensions, but assumes that $\langle p_t\rangle$ is regular as $r \to 2M$, even in the Schwarzschild background. Instead, our assumption is compatible with Eq. (11).

III. SEMICLASSICAL METRIC SOLUTION

A. Perturbative analytical solution

The leading order contributions of the stress-energy tensor are expected to behave as $\langle\rho\rangle \sim O(\hbar^1)$, $\langle p\rangle \sim O(\hbar^1)$ [where $\langle p\rangle = \langle p_r\rangle = \langle p_t\rangle$]. We can thus look for perturbative solutions of the semiclassical TOV equations, solving the system order by order in powers of $\hbar$. In this subsection we will obtain the first order correction using analytical techniques, and in the next subsection we will analyze the validity of this approach by solving the system of equations numerically.

Solving the TOV equations at order $\hbar^0$ gives $m(r) = M + O(\hbar)$ and $\phi \sim -\frac{1}{2}\log(1-2M/r) + O(\hbar)$, where M is an arbitrary constant of integration, which can be identified with the ADM mass. This is the Schwarzschild metric, as expected at order $\hbar^0$. To get something interesting we have to solve the equations at first order in $\hbar$. Let us define $m = M + m_1\hbar + O(\hbar^2)$, $\phi \sim -\frac{1}{2}\log(1-2M/r) + \phi_1\hbar + O(\hbar^2)$, $\langle\rho\rangle = \rho_1\hbar + O(\hbar^2)$, $\langle p\rangle = p_1\hbar + O(\hbar^2)$. Then the system of equations at first order in $\hbar$ is given by

$$\frac{dm_1}{dr} = 4\pi r^2\rho_1, \quad (12)$$

$$\frac{d\phi_1}{dr} = -\frac{m_1}{r^2 f^2} - \frac{4\pi r p_1}{f}, \quad (13)$$

$$\frac{dp_1}{dr} = -\frac{M}{r^2 f}(\rho_1 + p_1), \quad (14)$$

$$-\rho_1 + 3p_1 = \frac{M^2}{60\pi^2 r^6}, \quad (15)$$

where $f = 1 - \frac{2M}{r}$. This system can be solved analytically, obtaining the following expressions for the pressure and density[1]

$$\langle p \rangle = -\frac{\hbar M^3}{480\pi^2 r^7 f^2}\left(\frac{1}{7}+f\right) + \mathcal{O}(\hbar^2), \qquad (16)$$

$$\langle \rho \rangle = \hbar\left(-\frac{M^3}{160\pi^2 r^7 f^2}\left(\frac{1}{7}+f\right) - \frac{M^2}{60\pi^2 r^6}\right) + \mathcal{O}(\hbar^2), \quad (17)$$

and the following ones for the metric components

$$m = M + \frac{\hbar}{40320\pi M f}(9 - 36f\log(f) + 10f - 174f^2 + 246f^3 - 91f^4) + O(\hbar^2), \qquad (18)$$

$$\phi = -\frac{1}{2}\log f + \frac{\hbar}{80640\pi M^2 f^2}(3 + 36(-1 + 3f)f\log(f) - 35f + 152f^2 - 132f^3 + 5f^4 + 7f^5) + O(\hbar^2). \quad (19)$$

To fix the constants of integration we have assumed the natural boundary conditions $\langle p \rangle(r \to \infty) = 0$, $\langle \rho \rangle(r \to \infty) = 0$ and the metric tending to the Schwarzschild one as $r \to \infty$. For pedagogical purposes, we display the asymptotic form of the metric around $r = 2M$

$$ds^2 = -\left(f(r) - \hbar\left(\frac{1}{13440\pi M^2 f(r)} + \mathcal{O}(\log f)\right) + \mathcal{O}(\hbar^2)\right)dt^2 + \frac{dr^2}{f(r) - \hbar(\frac{1}{4480\pi M^2 f(r)} + \mathcal{O}(\log f)) + \mathcal{O}(\hbar^2)} + r^2 d\Omega^2. \quad (20)$$

In the Appendix we prove that the curvature at this singular point is finite, so this is just a coordinate singularity. In fact, this is just the classical Schwarzschild coordinate singularity at $r = 2M$ shifted to the value r_0 defined by $g_{rr}^{-1}(r_0) = 0$. Using the expression (18) and imposing $2m(r_0) = r_0$, we easily obtain

$$r_0 = 2M + \frac{\sqrt{\hbar}}{4\sqrt{70\pi}} + \mathcal{O}(\hbar). \qquad (21)$$

In geometrized units $\sqrt{\hbar} = l_p$ is the Planck length. This singular, limiting point defines the end of validity of our coordinate system, which would traditionally indicate the location of a "horizon" at $r = r_0$. However, note that, unlike the Schwarzschild case, in this point the component g_{tt} of the metric (the so called redshift function) does not vanish, but takes the value

$$g_{tt}(r_0) = -\frac{\sqrt{\hbar}}{12\sqrt{70\pi}M} + \mathcal{O}(\hbar). \qquad (22)$$

This implies that the static spacetime that we have obtained does not contain a horizon, i.e. it is not defining a black hole [34]. We check this in the Appendix.

Note that, even though (16) and (17) are generally very small (because of the prefactor $\hbar$), they become relevant around $r \sim r_0$, since in this limit the factor $f(r)$ in the denominator can compensate $\hbar$. In other words, quantum effects are quite important near the location of what was classically the horizon. The Krechtmann scalar is also found to be significantly corrected at the singular point

(see Appendix). These observations lead us to the following subsection.

B. Nonperturbative numerical solution

As we can see the results obtained above at first order in $\hbar$ also depend on $f(r)$, which takes values of order $\sqrt{\hbar}$ near the singular point $r = r_0$. This dependence compensates the small value of $\hbar$ in some expressions above. Because of this, a natural question is whether the perturbative method is a good approximation near to the singular point. To answer this we can solve the TOV equations at second order in $\hbar$ and analyze whether near the singular point the solution is consistent with the perturbative hypothesis (i.e. that the order $\hbar^1$ is larger than the order $\hbar^2$, etc.). The analysis is tedious and we avoid showing the details. What we obtain is that the $\hbar^2$ contribution to the pressure and the density is proportional to $\hbar^2/f(r)^4$. Near to the singular point $f(r)^4$ is of order $\hbar^2$, so this term competes with the first order contribution (16), which is proportional to $\hbar/f(r)^2$. Therefore we find that, near the singular point, the higher order contributions in $\hbar$ are not necessarily smaller than the first one and perturbation theory actually breaks down. Therefore, we cannot rely on the perturbative series in the vicinity of r_0 and we are forced to solve the differential TOV equations exactly, which can only be done numerically. Still, we shall find that the perturbative approach presented in the previous subsection is a good approximation to the problem, and it qualitatively predicts well the behavior of the nonperturbative solution.[2]

---

[1] The negative sign and the dependence on $1/f^2$ obtained in these expressions are in agreement with the exact results obtained on the fixed (Schwarzschild) background near the horizon for the Boulware vacuum state [see (11)].

[2] In this paper we work in the semiclassical regime in which fluctuations of the stress-energy tensor are negligible compared to its mean value. Going beyond this framework would require working with techniques in stochastic gravity [13], which is out of the scope of the present paper. By nonperturbative we mean the exact solution of the TOV equations within the semiclassical framework.
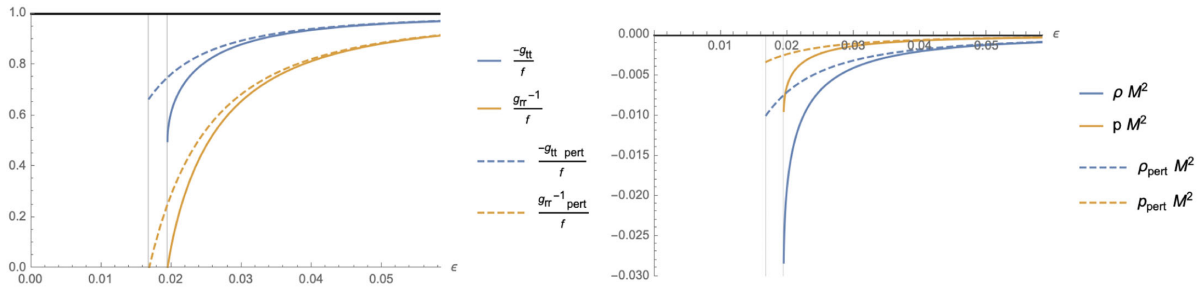
FIG. 1.   Numerical results obtained for the metric components and the renormalized energy density and pressure near the singular point $\epsilon = 0.01949$ (where $r = 2M + \epsilon\sqrt{\hbar}$). We have chosen $\hbar/M^2 = 10^{-5}$, but the plots do not change significantly for other values. We compare them with the perturbative solution (dashed curves), for which the singular point is $\epsilon = 0.01686$.

We now turn to solve numerically the TOV equations (4)–(6) using the equation of state (10) and $\langle p_r \rangle = \langle p_t \rangle$. We place the boundary conditions at $r = 1000M$, and demand that at this location the solution is approximately the Schwarzschild metric.[3] An important issue that one faces when solving the equations numerically is that the value of $\hbar$ is much smaller than M. To be able to distinguish the implications of a nonzero but tiny value of $\hbar$ from the numerical error, one needs a huge computer accuracy. To avoid this issue, a useful strategy is to use first some artificial high values of $\hbar$ (between $10^{-5}M^2$ and $10^{-15}M^2$), study the dependence of the results on $\hbar$, and then extrapolate the relevant quantities to the actual value of $\hbar$. By solving numerically the equations for different values of $\hbar$ and calculating for each case the value of r_0 we obtain results that approximately fit the expression $r_0 \approx 2M + 0.01947\sqrt{\hbar}$. This shift differs from the one estimated by the perturbative method ($r_0 \approx 2M + 0.01686\sqrt{\hbar}$) but the functional dependence on $\hbar$ remains the same.

In Fig. 1 we plot the components of the metric obtained numerically, normalized by the factor $f(r) = 1-2M/r$, as well as the renormalized energy density and pressure. They are plotted as a function of $\epsilon = \frac{r-2M}{\sqrt{\hbar}}$. With this new radial variable the singular point r_0 does not depend on the specific value of $\hbar$. These plots are taken for $\hbar/M^2 = 10^{-5}$, but we have analyzed them for other values and have seen that they do not significantly depend on the chosen value of $\hbar$ near the singular point. From these plots one can see that, as in the perturbative solution, the component g_{rr}^{-1} tends to 0 at the singular point $r = r_0$, while g_{tt} tends to a nonzero value. The energy density and pressure differ from 0 as they approach the singular point, as expected. More precisely $g_{tt} \sim O(\sqrt{\hbar}/M)$, $g_{rr}^{-1} \sim (r-r_0)/M$, $\rho \sim O(\hbar^0)$, and $p \sim O(\hbar^0)$ as $r \to r_0$. This is the same dependence on $\sqrt{\hbar}/M$ as that obtained by the perturbative approach, although the numerical coefficients are different. This allows us to

consider the perturbative solution as a qualitatively good approximation.

We can summarize the above numerical result in terms of the following generic expression for the metric

$$ds^2 = g_{tt}dt^2 + g_{rr}dr^2 + r^2 d\Omega^2, \qquad (23)$$

where $g_{rr}^{-1} \to 0$, as $r \to r_0 > 2M$ and $g_{tt}(r_0) \neq 0$. Furthermore, $g_{rr}^{-1} \sim (r-r_0)/M$ and $g_{tt}(r) \sim \mathcal{O}(\sqrt{\hbar}/M)$ in a neighborhood of r_0.

IV. EXTENSION BEYOND THE COORDINATE SINGULARITY

The metric (23) [or (20)] is only meaningful when $r > r_0$ because of the coordinate singularity at $r = r_0$. We recall (see Appendix) that the curvature scalars are finite at $r = r_0$. Physically this effective metric can be used to describe the exterior spacetime of a static, spherically symmetric star, including the vacuum polarization effects of quantum fields around. But in close analogy to the classical Schwarzschild case when expressed in $\{t, r, \theta, \phi\}$ coordinates, one may attempt to extend the spacetime across the $r = r_0$ point and examine if there exists a purely (quantum) vacuum solution. As remarked at the end of Sec. III A, the usual Eddington-Finkelstein coordinates fail to provide a regular metric, which prevents the usual analytical extension beyond $r = r_0$.

By looking at the specific form of the metrics (23) or (20) one realizes that they can be used to construct a portion of a static, traversable (and Lorentzian) wormhole [35,36]. By introducing the usual proper-length coordinate $l(r) \equiv \int_{r_0}^{r} 1/\sqrt{1 - 2m(r')/r'}dr' \geq 0$ the metric can be rewritten to fit the Morris-Thorne ansatz

$$ds^2 = -e^{-2\phi(l)}dt^2 + dl^2 + r(l)^2 d\Omega^2. \qquad (24)$$

Therefore, one can extend the spacetime beyond the critical point $r = r_0$ or $l = 0$ (which physically represents the throat of the wormhole) by analytically extending to negative values of l. The function $r = r(l)$ is determined

---

[3]To get more precision we can choose the corrected solution at first order in $\hbar$ obtained above, but the results near the singular point are numerically indistinguishable.

by inverting the equation $l = l(r)$ given above, but only when $l > 0$. For $l < 0$ the function $r = r(l)$ must be determined by other means.

A. Setup

Instead of working with the metric ansatz (2) and then transforming to (24) by a change of variables, we can alternatively solve the problem from scratch using the latter metric directly and explore if there exist wormhole solutions. The equivalent system of TOV equations now reads (we find convenient to introduce the defining relation $g(l) \equiv \frac{dr}{dl}$)

$$\frac{dr}{dl} = g, \tag{25}$$

$$\frac{dg}{dl} = \frac{1 - 8\pi r^2 \langle \rho \rangle + g^2}{2r}, \tag{26}$$

$$\frac{d\phi}{dl} = \frac{-1 - 8\pi r^2 \langle p_r \rangle + g^2}{2rg}, \tag{27}$$

$$\frac{d\langle p_r \rangle}{dl} = \frac{(-1 - 8\pi r^2 \langle p_r \rangle + g^2)(\langle p_r \rangle + \langle \rho \rangle)}{2rg}$$
$$+ \frac{2g(\langle p_t \rangle - \langle p_r \rangle)}{r}. \tag{28}$$

There are six unknowns for four equations. Again, we can impose two equations of state to get a solvable model. As before, we shall take $\langle p_t \rangle = \langle p_r \rangle$ (notice that the contribution of $\langle p_t \rangle - \langle p_r \rangle$ is negligible near the throat, where as we will see $g(0) = 0$) and $\langle T_a^a \rangle$ given by the trace anomaly:

$$-\langle \rho \rangle + 3\langle p \rangle$$
$$= \frac{\hbar}{180} \left[\frac{1 - g^2}{2\pi r^2} \left(3\frac{1 - g^2}{2\pi r^2} - 8\langle \rho \rangle \right) + 8\langle \rho \rangle (\langle p \rangle + \langle \rho \rangle) \right]. \tag{29}$$

To get wormhole solutions we must impose several conditions. Without loss of generality, we can locate the throat at $l = 0$. One of the sectors of the throat (that would represent the universe we live in) must be asymptotically flat, and inertial observers at infinity must measure time with t. We choose that sector corresponding to $l > 0$. Then the previous condition requires $\phi(\infty) = 0$, $\langle p_r \rangle(\infty) = \langle \rho \rangle(\infty) = 0$. On the other hand, the coordinate l should agree with the radial function $r(l)$ at infinity, i.e. $r(l) \to l$ as $l \to \infty$. Furthermore, for sufficiently large distances away from the throat, g must be given by the Morris-Thorne coordinate transformation (the solution should mimic a hole at large distances), i.e. $g(l) \sim \sqrt{1 - 2m(l)/l}$ and therefore $g(\infty) = 1$.

This set of boundary conditions, together with the two equations of state specified above, can be used to obtain a unique solution to the above system of differential equations, integrating all the way down from $l = +\infty$ until negative values of l. Notice that in general there will be no mirror-reflection symmetry at the throat. The results are shown in the next subsection. For the solution to represent a wormhole, note that (i) the throat must have a finite, nonvanishing radius, so $r(0) = r_0 > 0$, and (ii) the throat area must correspond to a minimum, therefore $g(0) = 0$.

Before discussing the results, we remark an important issue. It may seem that the above system of equations is not well defined at the throat $l = 0$ because of $g(0) = 0$ in the denominator of some equations. But notice that, according to Einstein's equation,

$$\langle p_r(r) \rangle = -\frac{1}{8\pi} \left[\frac{2m}{r^3} - 2\left(1 - \frac{2m}{r} \right) \frac{\partial_r \phi}{r} \right], \tag{30}$$

so at the throat (where $2m(r) = r$) we also have $p_r(0) = -1/(8\pi r_0^2)$, provided that $\partial_r \phi(0)$ is well-defined at the throat or that it does not blow up as quickly as $(1 - 2m/r)^{-1}$ (this is verified in this case, using the numerical solution obtained in the previous section one can see that $\partial_r \phi \sim (1 - 2m(r)/r)^{-1/2}$ when $r \to r_0$).
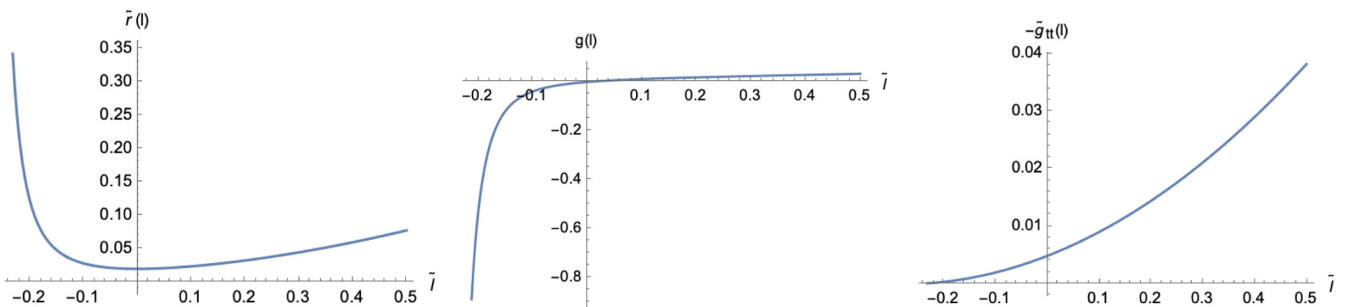

FIG. 2. Numerical results obtained for the components of the metric (24) and $g(l) = r'(l)$ in terms of $\tilde{l} = l\hbar^{-1/4}M^{-1/2}$. The represented interval of $\tilde{l}$ includes the throat ($\tilde{l} = 0$) and the curvature singularity ($\tilde{l} \approx -0.278$). We have defined the quantities $\tilde{r} = (r - 2M)\hbar^{-1/2}$ and $\tilde{g}_{tt} = g_{tt}\hbar^{-1/2}M$, in such a way that their values at the throat do not depend on the chosen value of $\hbar$. We have chosen $\hbar/M^2 = 10^{-3}$ for these plots, but they have a similar form for other values.

Therefore, the numerator of (27) and (28) also vanishes whenever the denominator does, and we have a 0/0 ambiguity. To ensure that we can extend the metric across the throat one needs to check first that the limit $l \to 0$ tends to a finite value under the boundary conditions specified above. Numerically we find that near the throat $1 + 8\pi r^2 p \sim O(l)$ and $g \sim O(l)$, so we can conclude that the limit of the quotient will be finite.

B. Results

In Fig. 2 we show the result of solving numerically the system of equations (25), (26), (27), (28) and (29) under the conditions specified in the previous subsection. As in Sec. III. B, to capture the implications of a nonvanishing but tiny value of $\hbar$ on the equations, we do the calculation for several high values of $\hbar$ (so that their effect is numerically distinguishable), then we perform a fit of the results to be able to extrapolate the value of interest with the actual value of Planck's constant. In our calculation the throat is located at $l = 0$, note how at this point there is a bounce in the function $r(l)$ (its derivative $g(l)$ changes sign).

Furthermore, we find that in the interior region, $l < 0$, a new singular point appears at $l_s \sim -0.278\hbar^{1/4}\sqrt{M}$. It is a singular point because the redshift function vanishes there, $g_{tt}(l_s) = 0$. As we approach to l_s we find that the renormalized density, the pressure and the scalar of curvature $R = 8\pi(-\rho + 3p)$ all tend to diverge. This signals the existence of a curvature singularity. To confirm the existence of this singularity from an analytical viewpoint we can examine the expression of the scalar curvature in terms of the metric components:

$$R(l) = \frac{g'_{tt}(l)^2}{2g_{tt}(l)^2} - \frac{g''_{tt}(l)r(l) + 2g'_{tt}(l)r'(l)}{g_{tt}(l)r(l)} - \frac{2(2r(l)r''(l) + r'(l)^2 - 1)}{r(l)^2}. \quad (31)$$

Since at the singular point $g_{tt}(l_s) = 0$ (see Fig. 2) some terms of this expression diverge at this point. Although $g'_{tt}(l)$ also vanishes at $l = l_s$, numerical computations show that it decreases slower than $g_{tt}(l)$. To see the causal character of this curvature singularity, let us consider the induced metric on a $l =$ constant three-dimensional hypersurface: $d\bar{s}^2 = g_{tt}(l)dt^2 + r(l)^2 d\Omega^2$. At the singularity $l = l_s$ we have $g_{tt}(l_s) = 0$, so the metric becomes degenerate: $d\bar{s}^2 = 0 + r(l_s)^2 d\Omega^2$. Therefore, the surface $l = l_s$ becomes a null hypersurface [37], and this curvature singularity is null. Figure 3 provides a Penrose diagram that shows all these features.

An important question is how long it would take for an observer crossing the throat to reach this curvature singularity. To study this let us consider a radial and time-like geodesic starting at $l = 0$ (throat) and ending at the singular
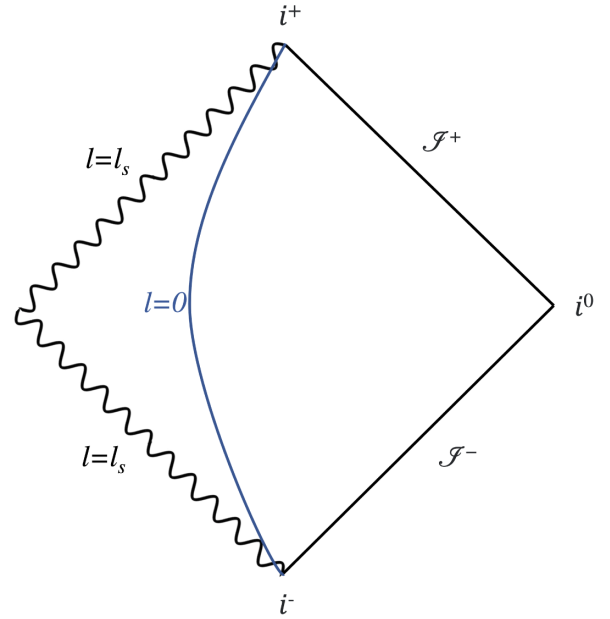

FIG. 3. Penrose diagram showing the wormhole throat ($l = 0$) and the null curvature singularity ($l = l_s$).

point $l = l_s$. The relevant geodesic equation for a static and spherically symmetric metric $ds^2 = g_{tt}(l)dt^2 + g_{ll}(l)dl^2 + r(l)^2 d\Omega^2$ is given by

$$\frac{dl}{d\tau} = \pm\sqrt{-g_{ll}^{-1}\left(E^2 g_{tt}^{-1} + \frac{L^2}{r^2} + \mu\right)} \quad (32)$$

where τ is the proper time, $\mu = +1, 0, -1$ for timelike, null and spacelike geodesics respectively, and E and L are constants of motion given by $E = -g_{tt}\frac{dt}{d\tau}$ and $L = r^2\frac{d\phi}{d\tau}$. In our case $g_{ll} = 1$, $\mu = 1$, $L = 0$, and $dl/d\tau < 0$ (the geodesic is approaching the singularity), so

$$\frac{dl}{d\tau} = -\sqrt{E^2 g_{tt}(l)^{-1} - 1}. \quad (33)$$

The proper time needed to reach the curvature singularity from the throat is then given by

$$\Delta\tau = -\int_0^{l_s} \frac{dl}{\sqrt{E^2 g_{tt}(l)^{-1} - 1}}. \quad (34)$$

(the condition that the geodesic propagates into the future, $\partial_\tau t > 0$, implies $E^2 g_{tt}(l)^{-1} > 1$ and guarantees that the integral is real). The order of magnitude of this quantity can be estimated as follows. From (22) we know that $g_{tt}(0) \sim \sqrt{\hbar}/M$. Assuming $E \sim 1$, we have $E^2 g_{tt}^{-1}(l) \gg 1$ in the region of the integration. Since $|l_s| \sim \hbar^{1/4}\sqrt{M} \ll 1$ we can also Taylor expand the integral to finally get

$$\Delta\tau \sim -\int_0^{l_s} \sqrt{g_{tt}(l)}dl \sim \sqrt{g_{tt}(0)}|l_s| + O(l_s^2) \sim \sqrt{\hbar} \quad (35)$$

So an observer crossing the throat will almost immediately see the presence of the curvature singularity.

Finally, we want to stress that the occurrence of the curvature singularity has been obtained for a purely vacuum semiclassical solution. The presence of matter producing very compact stellar objects (ECOs) makes only the outer part of the solution physically relevant. Moreover, these results also suggest a maximum in the compactness of ECOs. This maximum would be given by the minimum of the radial function $r(l)$, i.e. the throat ($r = r_0$). Therefore this maximum of compactness [measured as $2M/r(l)$] is of order

$$\frac{2M}{r_0} \sim 1 - 0.01686\frac{\sqrt{\hbar}}{2M}. \quad (36)$$

We regard (36) as one of the main results of this work. Probing the exterior of the semiclassical metric via scalar and vector perturbations will be the topic of the next section.

Remark: Another way to extend the metric beyond the coordinate singularity $r = r_0$ consists in defining a coordinate $\bar{r}$ by $\frac{d\bar{r}}{dr} = e^{-\phi(r)}(1 - \frac{2m(r)}{r})^{-1/2}$. In this case the metric has the form

$$ds^2 = -G(\bar{r})dt^2 + \frac{dr^2}{G(\bar{r})} + R(\bar{r})^2 d\Omega^2. \quad (37)$$

Using this metric as an ansatz for solving the semiclassical TOV equations we found that the functions G and R can be analytically extended beyond the coordinate singularity $\bar{r} = \bar{r}_0$. In particular $R(\bar{r})$ reaches a minimum at $\bar{r}_0$ and starts increasing for lower values, as expected for a wormhole metric. On the other hand $G(\bar{r})$ continues to decrease until it reaches the value $\bar{r} = \bar{r}_s$, where $G(\bar{r}_s) = 0$. At this point we again find a curvature singularity, which is equivalent to the one found in the other extension explained above. Therefore, with this alternative extension, we obtain the same conclusions. However the approach described above allows a higher accuracy in the numerical calculations.

V. PROPAGATION OF WAVES IN THE SEMICLASSICAL METRIC

The propagation of waves on a given spacetime background provides a way to test some features of this metric by studying the scattering properties of the wave. Furthermore, they provide a means to test the stability of the metric under linear perturbations, which is a necessary condition for any semiclassical metric that aims to describe acceptable astrophysical systems. In this section we will study scalar and electromagnetic perturbations around the semiclassical metric constructed in Sec. III. In particular, we will compute the leading order corrections to the light-ring frequency modes. These frequencies depend only on the geometry around the light-ring of the classical black hole, and describe the early ringdown stage in gravitational wave observations of binary mergers. While the late ringdown stage is expected to be described by the proper QNM frequencies [38,39], the calculation of these is out of the scope of the present paper.

A. Scalar perturbations

Let us study the behavior of a massless scalar field coupled to a general static and spherically symmetric background, $ds^2 = g_{tt}dt^2 + g_{rr}dr^2 + r^2 d\Omega^2$. The field satisfies the Klein-Gordon equation

$$(\Box + \xi R)\phi = 0. \quad (38)$$

Since the metric is static and spherically symmetric, we can look for solutions of the following form

$$\phi_{\omega lm} = \frac{1}{r}e^{-i\omega t}Y_{lm}(\theta, \psi)\Psi_{\omega l}(r). \quad (39)$$

For a curved spacetime the D'Alembert operator is given by $\Box\phi = \frac{1}{\sqrt{-g}}\partial_\mu(\sqrt{-g}g^{\mu\nu}\partial_\nu\phi)$. The Klein-Gordon equation decouples and, after some calculations one obtains the following equation for the radial function

$$F^2\Psi_{\omega l}'' + FF'\Psi_{\omega l}' + (\omega^2 - V_l)\Psi_{\omega l} = 0, \quad (40)$$

where

$$F(r) = \sqrt{-\frac{g_{tt}}{g_{rr}}}, \quad (41)$$

$$V(r) = -g_{tt}(r)\left(\frac{l(l+1)}{r^2} - \xi R(r)\right) + \frac{F(r)F'(r)}{r}. \quad (42)$$

If we define a generalized tortoise coordinate as $\partial_{r^*} = F(r)\partial_r$, then Eq. (40) can be rewritten in the usual Regge-Wheeler form $\partial_{r_*}^2\Psi_{\ell m} + (\omega^2 - V)\Psi_{\ell m} = 0$. In particular, for a Schwarzschild background we recover the usual expression.

Now let us study this potential for our particular case, given by $g_{tt} = -e^{-2\phi(r)}$ and $g_{rr} = 1 - \frac{2m(r)}{r}$, where $\phi(r)$ and $m(r)$ have been obtained in Sec. III. Using the semiclassical TOV equations we can rewrite the potential as

$$V(r) = e^{-2\phi(r)}\left(\frac{l(l+1)}{r^2} + \frac{2m(r)}{r^3} + 4\pi((1-6\xi)\langle p(r)\rangle \right.$$
$$\left. + (-1+2\xi)\langle\rho(r)\rangle)\right). \quad (43)$$

It is easy to see that in the Schwarzschild limit $\hbar \to 0$ this expression reduces to the usual effective potential for scalar fields. We can now use the perturbative solution of the corrected Schwarzschild metric to obtain the correction of the Regge-Wheeler potential at first order in $\hbar$. The resulting expression, at first order in $\hbar$, yields

$$V(r) = V_0(r) + \frac{\hbar}{20160\pi M^2 r^6 f}[-2688M^4\xi f^2$$
$$+ Mr^3(-3\lambda + (53 + 32\lambda)f - 40(1 + 3\lambda)f^2$$
$$+ 12(-36 + \lambda)f^3 + (664 + 7\lambda)f^4 - 245f^5)$$
$$+ 18r^4((1 + \lambda) - (5 + 3\lambda)f + 4f)f\log(f)]$$
$$+ O(\hbar^2), \tag{44}$$

where $f = 1 - \frac{2M}{r}$, $\lambda = l(l + 1)$ and $V_0(r) = f(\frac{\lambda}{r^2} + \frac{2M}{r^3})$, which is the effective potential for scalar fields on a Schwarzschild background. Note that this expression does not depend on ξ. This is because the scalar curvature is given by $R = 8\pi(-\rho + 3p)$, and expanding around $r = 2M$ we have $\rho \approx 3p$ at leading order [see (17) and (16)], so the term ξR is subleading. On the other hand, near the throat $f(r_0) \sim O(\sqrt{\hbar}/M)$ so the quantum correction of the effective potential is of order $O(\sqrt{\hbar}/M^3)$ near the throat, while it is of order $O(\hbar/M^4)$ in general.

Using this expression for the corrected effective potential, we can now obtain the quantum corrections at first order in $\hbar$ to the light ring frequencies. The computation of these frequencies requires numerical methods. However, one can obtain a reasonable estimation by using the WKB approximation [40].

Let us briefly review the calculation for a Schwarzschild metric. In this framework the light ring frequencies at 0th adiabatic order are given by

$$\omega_n^2 = V(r_m^*) - i\sqrt{-2V''(r_m^*)}\left(n + \frac{1}{2}\right), \tag{45}$$

where r_m^* is the value of the tortoise coordinate at which the potential is maximum, and the primes mean derivatives with respect to r^*. In the case of a Schwarzschild background the maximum of the potential is located at

$$r_m = \frac{3(\lambda - 1) + \sqrt{(9\lambda + 14)\lambda + 9}}{2\lambda}M, \tag{46}$$

which for large l tends to $r_m \sim 3M$. [The case $\lambda = 0$ ($l = 0$) has to be studied separately, we analyze it at the end of this section]. Using this expression, we can obtain the frequency of the light-ring modes for a scalar perturbation in a classical black hole

$$\omega_{\text{Sch}}^2 = \frac{1}{M^2}\left(1 - \frac{2}{\tilde{r}_m}\right)\left(\frac{\lambda}{\tilde{r}_m^2} + \frac{2}{\tilde{r}_m^3}\right) - i\left(n + \frac{1}{2}\right)\frac{2}{M^2\tilde{r}_m^4}\sqrt{\left(1 - \frac{2}{\tilde{r}_m}\right)(-96\tilde{r}_m - 10(3\lambda - 7)\tilde{r}_m^2 + 4(5\lambda - 3)\tilde{r}_m^3 - 3\lambda\tilde{r}_m^4)}, \tag{47}$$

where $\tilde{r}_m = r_m/M$.

Now let us see how this expression changes if we add quantum corrections at first order in $\hbar$. The corrected effective potential (44) has its maximum at $r = r_m + \frac{\hbar}{M}\epsilon + O(\hbar^2)$, where

$$\epsilon = \frac{1}{5040\pi}\tilde{r}_m^{-4}(40 + 12(\lambda - 1)\tilde{r}_m - 3\lambda\tilde{r}_m^2)^{-1}\left(1 - \frac{2}{\tilde{r}_m}\right)^{-2}\left[-392(48\xi - 35) + 8(21\lambda + 3360\xi - 2663)\tilde{r}_m\right.$$
$$- 2(249\lambda + 6384\xi - 5057)\tilde{r}_m^2 + 12(6\lambda + 168\xi - 59)\tilde{r}_m^3 + 3(89\lambda - 177)\tilde{r}_m^4 + 27(3 - 5\lambda)\tilde{r}_m^5 + 18\lambda\tilde{r}_m^6$$
$$+ \frac{9}{2}\tilde{r}_m^5(-32 - 9(\lambda - 1)\tilde{r}_m + 2\lambda\tilde{r}_m^2)\left(1 - \frac{2}{\tilde{r}_m}\right)^2\log\left(1 - \frac{2}{\tilde{r}_m}\right)\right]. \tag{48}$$

Using the equation (45) we obtain the following expression for the corrected frequencies at first order in $\hbar$

$$\text{Re}[\omega^2] = \text{Re}[\omega_{\text{Sch}}^2] + \frac{\hbar}{630\pi M^4}\frac{336(\lambda + 2)\xi - 201\lambda - 560 + \tilde{r}_m(-84(\lambda + 3)\xi + 13\lambda^2 + 42\lambda + 210)}{\lambda\tilde{r}_m^8(1 - \frac{2}{\tilde{r}_m})} + O(\hbar^2). \tag{49}$$

$$\mathrm{Im}[\omega^2] = \mathrm{Im}[\omega_{\mathrm{Sch}}^2] - \frac{\hbar}{2520\pi M^4}\left(n+\frac{1}{2}\right)\tilde{r}_m^{-8}\left(1-\frac{2}{\tilde{r}_m}\right)^{-3/2}(-96\tilde{r}_m - 10(3\lambda-7)\tilde{r}_m^2 + 4(5\lambda-3)\tilde{r}_m^3 - 3\lambda\tilde{r}_m^4)^{-1/2}$$

$$\cdot\left[1176(144\xi-125) + 12\tilde{r}_m(-749\lambda - 25760\xi + 645120\pi\tilde{r}_m\epsilon + 23011)\right.$$

$$+ 4\tilde{r}_m^2(3977\lambda + 52584\xi + 25200\pi(21\lambda-121)\tilde{r}_m\epsilon - 45476)$$

$$- 2\tilde{r}_m^3(3468\lambda + 31584\xi + 25200\pi(63\lambda-139)\tilde{r}_m\epsilon - 20771)$$

$$+ 2\tilde{r}_m^4(-1069\lambda + 3528\xi + 5040\pi(170\lambda-171)\tilde{r}_m\epsilon + 1956) - 9\tilde{r}_m^5(-271\lambda + 560\pi(77\lambda-30)\tilde{r}_m\epsilon + 312)$$

$$+ 9\tilde{r}_m^6(-71\lambda + 3360\pi\lambda\tilde{r}_m\epsilon + 30) + 54\lambda\tilde{r}_m^7 + \frac{9}{2}\tilde{r}_m^4(-768 - 14(15\lambda-59)\tilde{r}_m - 6(47-35\lambda)\tilde{r}_m^2 - 5(13\lambda-6)\tilde{r}_m^3$$

$$\left. + 6\lambda\tilde{r}_m^4)\left(1-\frac{2}{\tilde{r}_m}\right)\log\left(1-\frac{2}{\tilde{r}_m}\right)\right] + O(\hbar^2). \tag{50}$$

As mentioned above, the case $l = 0$ requires special attention. In this case the effective potential has its maximum at

$$r = \frac{8M}{3} + \frac{\hbar}{430080\pi M}(1008\xi - 1767 + 2048\log(2)) + O(\hbar^2). \tag{51}$$

Therefore, the corrected frequency at first order in $\hbar$ for $l = 0$ is given by

$$\omega^2 = \omega_{\mathrm{Sch}}^2 + \frac{3\hbar}{286720\pi M^2}((336\xi - 241)\mathrm{Re}[\omega_{\mathrm{Sch}}^2] - 2i(336\xi - 5)\mathrm{Im}[\omega_{\mathrm{Sch}}^2]) \tag{52}$$

One can see that, even if the geometry of the spacetime is drastically changed by quantum effects near to the horizon, they do not imply significant corrections to the physical observables in the exterior region.

B. Electromagnetic perturbations

Let us now study the propagation of electromagnetic waves on a general static and spherically symmetric metric given by $ds^2 = g_{tt}(r)dt^2 + g_{rr}(r)dr^2 + r^2d\Omega^2$. The electromagnetic field F_{ab} satisfies the source-free Maxwell equations:

$$\nabla_a F^{ab} = 0, \qquad \nabla_a {}^*F^{ab} = 0, \tag{53}$$

where ${}^*F$ is the Hodge dual of F. The second equation is solved with $F_{ab} = A_{a,b} - A_{b,a}$, where A_a is the electromagnetic potential, and the problem is reduced to solve the first equation above for the vector field A_a. For a spherically symmetric background spacetime we can search for solutions by expanding A_a in the basis of 4-dimensional vector spherical harmonics $(Y_a)_{\ell m}$. Elements of this basis are classified according to their behavior under parity transformations. For axial/odd modes, which have parity $(-1)^{\ell+1}$, the electromagnetic potential can be expanded as

$$A_a^-(t,r,\theta,\phi) = \sum_{\ell,m}\begin{bmatrix} 0 \\ 0 \\ \frac{a^{lm}(t,r)}{\sin\theta}\partial_\phi Y_{lm} \\ -a^{lm}(t,r)\sin\theta\partial_\theta Y_{lm} \end{bmatrix}, \tag{54}$$

for some (gauge-invariant) coefficients $a^{lm}(t,r)$. Using this ansatz one can check that there is only one nontrivial independent equation from $\nabla_a F^{ab} = 0$. For a static spacetime we can further separate $a_{\ell m} = e^{-i\omega t}\Psi_{\ell m}^-(r)$, and the resulting equation can be written as

$$F^2\Psi_{\ell m}^{-\prime\prime} + FF'\Psi_{\ell m}^{-\prime} + (\omega^2 - V_l)\Psi_{\ell m}^- = 0, \tag{55}$$

where

$$F(r) = \sqrt{-\frac{g_{tt}}{g_{rr}}}, \tag{56}$$

$$V_l(r) = -g_{tt}(r)\frac{l(l+1)}{r^2}. \tag{57}$$

Again, introducing the tortoise coordinate by $\partial_{r^*} = F(r)\partial_r$, one recovers the usual Regge-Wheeler form of the equation, $\partial_{r_*}^2\Psi_{\ell m}^- + (\omega^2 - V_\ell)\Psi_{\ell m}^- = 0$. In particular, for a Schwarzschild background we recover the usual expression.

For polar/even modes, which have parity $(-1)^\ell$, the electromagnetic potential can be expanded as

$$A_a^+(t,r,\theta,\phi) = \sum_{\ell,m}\begin{bmatrix} f^{lm}(t,r)Y_{lm} \\ h^{lm}(t,r)Y_{lm} \\ k^{lm}(t,r)\partial_\theta Y_{lm} \\ k^{lm}(t,r)\partial_\phi Y_{lm} \end{bmatrix}, \tag{58}$$

for some coefficients f^{lm}, h^{lm}, k^{lm}. However, these coefficients are gauge-dependent. Let us introduce the three gauge-invariant combinations $\Psi^+ = \sqrt{-g_{tt}g_{rr}}\frac{r^2}{\ell(\ell+1)} \times (\partial_t h^{lm} - \partial_r f^{lm})$, $\Psi_{1,\ell m} = f^{lm} - \partial_t k^{lm}$ and $\Psi_{2,\ell m} = h^{lm} - \partial_r k^{lm}$ (these combinations are essentially the field components F_{tr}, $F_{t\phi}$, $F_{r\phi}$, respectively; the rest of the field components are redundant). Using Maxwell equations one can conclude, after some work, that $\Psi^+_{\ell m}$ satisfies the same equation (55) as the axial solution $\Psi^-_{\ell m}$, and the rest of the field variables are determined from it: $\Psi_1 = -\frac{\partial_r \Psi^+}{g_{rr}} + \frac{\partial_r(g_{tt}g_{rr})}{2g_{tt}g_{rr}^2}\Psi^+$ and $\Psi_2 = \frac{\partial_t \Psi^+}{g_{tt}}$. One can easily check that these results fully solve the system of equations $\nabla_a F^{ab} = 0$, and the whole problem reduces to solve (55) with suitable boundary conditions.

The fields $\Psi^\pm_{\ell m}$ constitute the two fundamental degrees of freedom per spacetime point of the electromagnetic field. Notice that both fields satisfy exactly the same dynamical equation even when the quantum corrections considered in this paper are included, leading in particular to the usual phenomenon of isospectrality [41]. This could have been guessed in advance from the electric-magnetic duality symmetry of the source-free Maxwell equations [42], since Ψ^+ plays the role of the electric field while Ψ^- represents the magnetic degree of freedom.

For the perturbative corrected Schwarzschild metric provided in Sec. III, the first order correction in $\hbar$ to the potential yields

$$V(r) = V_1(r) - \frac{\hbar l(l+1)}{5040\pi M^2 r^7}\left(\frac{2M}{f(r)}(21M^2 r^2 + 40M^3 r\right.$$
$$- 14M^4 - 36Mr^3 + 9r^4) + 9r^4(r - 3M)\log(f(r))\bigg)$$
$$+ O(\hbar^2), \tag{59}$$

where $V_1 = f(r)\frac{l(l+1)}{r^2}$ is the potential for electromagnetic perturbations on the Schwarzschild metric, and $f(r) = 1 - \frac{2M}{r}$. As in the scalar case, for $r \to r_0$ the effective potential acquires a nonzero residual value of order $\sqrt{\hbar} = \ell_p$, which is not present in the classical case.

Finally, let us analyze the quantum corrections to the light ring frequencies of electromagnetic perturbations, again using the WKB approximation described above. For the Schwarzschild metric the maximum of the Regge-Wheeler potential is located at $r = 3M$, and therefore using the expression (45) one obtains

$$\omega^2_{\text{Sch}} = \frac{l(l+1)}{27M^2} - i\frac{2\sqrt{l(l+1)}}{27M^2}\left(n + \frac{1}{2}\right). \tag{60}$$

For our (perturbatively) corrected spacetime, at first order in $\hbar$ we obtain the maximum of the potential (59) at $r = 3M + \frac{\hbar}{90720\pi M}(243\log(3) - 20)$. Substituting in (45)

and expanding in Taylor series we obtain the following expression for the quantum correction to the light ring frequencies:

$$\omega^2 = \omega^2_{\text{Sch}} + \frac{\hbar}{17010\pi M^2}(-13\text{Re}[\omega^2_{\text{Sch}}] + 11i\text{Im}[\omega^2_{\text{Sch}}]). \tag{61}$$

Again, the quantum effects of vacuum polarization do not lead to significant, observable corrections.

VI. SUMMARY AND FINAL COMMENTS

The theory of test quantum fields in a given gravitational background is widely regarded as a useful and fruitful framework for exploring quantum fluctuations enhanced by gravity. This theory can be further used to analyze the backreaction of these quantum effects on the spacetime background by looking at the semiclassical Einstein's equations (1). Solving these equations is, however, a very elusive problem and only in very highly symmetric situations one can carry out the computation in a manageable way. A good example are conformally flat spacetimes with conformal matter fields. In this case $\langle T_{ab}\rangle$ is essentially characterized by the conformal anomaly. Another relevant example emerges in two-dimensional dilaton-gravity models coupled to conformal matter. The conformal anomaly in two dimensions fully determines the quantum stress tensor for a given choice of the vacuum state, thus allowing us to solve analytically the semiclassical backreaction equations for a relevant class of two-dimensional models [17].

In this paper we have reanalyzed the four-dimensional problem from scratch, focusing on static and spherically-symmetric backgrounds. The general expressions given in [14] for the renormalized stress tensor, when the quantum field lives in static and spherically symmetric spacetimes, represent a very significant progress, but they are still quite involved and unpractical to solve the semiclassical equations. One way to simplify the problem is to restrict ourselves to conformal matter and take advantage of the trace anomaly. However, those assumptions (spherical symmetry, staticity and conformal matter) are still not sufficient to reduce the problem to a manageable form, in sharp contrast with the effective two-dimensional case [18–20]. To overcome this difficulty we have introduced an extra simplifying assumption, suggested by well-known results in the fixed Schwarzschild background. Since we are mainly interested in the behavior of the geometry in the very near horizon region $r \sim 2M$ (in the macroscopic vicinity of $2M$ one does not expect any significant modification of the classical Schwarzschild geometry) we have assumed the exact relation between $\langle p_t\rangle$ and $\langle p_r\rangle$ in the vicinity of the classical horizon (suggested by the results in the fixed background approach). Our findings appear to be essentially insensitive of this assumption. More precisely, we have numerically checked that the (nonperturbative) backreaction solution obtained

with other restrictions (such as $\langle p_t \rangle = 0$) are qualitatively similar to those described in Sec. III. Furthermore, our results do not depend on the particular form of the conformal matter either (for a massless Dirac field we have obtained results similar to those for a scalar field).

One remarkable property of the semiclassical backreaction solution obtained in Secs. III and IV is that the radial function can never reach 0 (where the classical curvature singularity is located), but rather it has a minimum on a time-like surface. This mimics the throat of an (asymmetric) wormhole, and it is located at $r_0 \approx 2M + \mathcal{O}(\sqrt{\hbar})$, where the red-shift function reaches a very small but nonzero value.[4] Beyond this bouncing surface for the radial function we have found a null curvature singularity at a finite proper-time distance (of order $\mathcal{O}(\sqrt{\hbar})$ from the throat). The overall physical picture qualitatively agrees with the results obtained from the purely two-dimensional approach. This indicates that the two-dimensional approach could be more accurate than it could be expected.

The global picture obtained from this semiclassical framework differs drastically from its counterpart in classical general relativity, specially regarding the black hole interior region. Strictly speaking, here the classical horizon disappears and it is replaced by a bouncing timelike surface, beyond which a null curvature singularity emerges immediately. The underlying reason for this seems to be rooted in the singular behavior of the renormalized stress tensor at the classical horizon obtained in the fixed background approach. In light of these results, it looks as if the original singular behavior of the stress-tensor in the classical horizon manifests itself in the metric in the form of a curvature singularity as a result of the backreaction. We regard this singularity as a side effect of the assumption of a pure vacuum solution. The presence of matter could tame the singularity if vacuum polarization effects continue to be relevant (as suggested by the results in [23]) and allow the formation of ECO's. However in this case the maximum compactness of these objects is bounded by $2M/r_0 \sim 1 - 0.01686\sqrt{\hbar}/(2M)$. This bound is a direct consequence of the fact that the exterior geometry of ECOs has to be described by the external portion of our semiclassical solution, and not by the classical Schwarzschild metric.

We have also analyzed potential physical implications of the quantum corrected geometry in the exterior region. In Sec. V we have analyzed in detail the scalar and electromagnetic perturbations, paying special attention to the so-called "light ring frequencies," which are the relevant observables in the ringdown of binary black holes. We have evaluated the corrected light ring frequencies using our

---

[4]We note that the power in the dependence on $\hbar$ is different from that obtained in the approach of Ref. [24], for which $r_0 \approx 2M + \mathcal{O}(\hbar)$. Furthermore, we also have discrepancies in the analytic form of the metric components.

predictions for the semiclassical metric, and they differ from their classical counterpart by corrections of order $\mathcal{O}(\hbar/M^2)$. Somewhat not surprising, the drastic modification of the metric around the classical horizon does not lead to observable corrections on these observables, since these frequencies are determined by the spacetime curvature around the light-ring. To really probe the quantum corrections around the classical horizon geometry one would need to compute the proper BH quasinormal mode frequencies of the system, which would most likely differ nonperturbatively from the classical BH QNMs. However these observables require the specification of boundary conditions at the center or surface of the quantum object in question, and this is out of the scope of the present paper.

We plan to extend this work in several directions. Apart from computing the QNM frequencies above, our goal is to analyze the inclusion of collapsing matter and the impact of the time-dependent phase on the backreaction effects. This is indeed a very difficult problem in the four-dimensional arena and requires a separate study.

Note added.—After the communication of this paper another work appeared [43] which confirms some of our conclusions, giving further support to our results.

APPENDIX: NATURE OF THE SINGULAR POINT $r = r_0$

In this appendix will analyze in detail the nature of the singular point $r = r_0$ obtained in Sec. III and will prove that it is a coordinate singularity. We will also see why this singular point does not define a classical horizon.

Let us consider a general metric of the form

$$ds^2 = -G(r)dt^2 + \frac{dr^2}{F(r)} + r^2 d\Omega^2, \qquad (A1)$$

with $G(r) > 0$ and $F(r) > 0$. Its corresponding curvature scalar is given by

$$R = \frac{4G^2(rF' + F - 1) + rG(G'(rF' + 4F) + 2rFG'') - r^2F(G')^2}{2r^2G^2}. \tag{A2}$$

In our case $F(r_0) = 0$ at the singular point, but $G(r_0) \neq 0$ and their derivatives are not divergent, so the scalar curvature is finite at this point, and therefore $r = r_0$ is a coordinate singularity. This statement can also be inferred from a perturbative analysis of the semiclassical Einstein's equations $R = 8\pi\langle T_a^a \rangle$, since at first order the trace does not diverge $[\langle T_a^a \rangle = \frac{\hbar M^2}{60\pi^2 r^6} + O(\hbar^2)]$.

Another way to confirm this, and to assess the impact of the quantum-vacuum polarization on the classical Schwarzschild geometry, is by analyzing the Kretschmann curvature scalar. For a static and spherically symmetric metric, the explicit expression can be simplified considerably if we use the TOV equations. It reads

$$K(r) = 16\left(-\frac{8\pi m(r)\langle\rho(r)\rangle}{r^3} + \frac{3m(r)^2}{r^6} + 4\pi^2[2\langle p(r)\rangle\langle\rho(r)\rangle + 3\langle p(r)\rangle^2 + 3\langle\rho(r)\rangle^2]\right) \tag{A3}$$

Since the renormalized pressure and density are of order $\hbar/f^2$ near the singular point (i.e. numerically of order ~ 1 since $f(r_0) \sim \sqrt{\hbar}$), we can see that the Kretschmann scalar does not diverge. In particular, by substituting the perturbative solution at first order in $\hbar$ into this expression we obtain

$$K(r) = \frac{48M^2}{r^6} + \frac{\hbar}{105\pi r^9}\left(\frac{2M}{r^2f(r)^2}\left(728M^4 - 818M^3 r + 212M^2 r^2 + 27Mr^3 - 9r^4\right) - 9r^3\log\left(1 - \frac{2M}{r}\right)\right) + O(\hbar^2). \tag{A4}$$

As mentioned above, near the singular point the leading correction to the Kretschmann scalar behaves as $\hbar/f^2$, which tends to $O(1)$ at this point. Notice that, as compared to the classical Schwarzschild value, the Kretschmann scalar is expected to receive corrections that are of order $O(\hbar^0)$ in a neighborhood of the singular point, meaning that quantum corrections may be significant for the nearby geometry despite the tiny value of $\hbar$.

If we substitute the equation of state (10) in (A3), we see that the terms that include the trace anomaly are of order $\hbar$ near the singular point, so for a conformal quantum field we can further approximate the Kretschmann scalar as

$$K(r) \sim 16\left(-\frac{8\pi m(r)\langle\rho(r)\rangle}{r^3} + \frac{3m(r)^2}{r^6} + 16\pi^2\langle\rho(r)\rangle^2\right) \tag{A5}$$

As mentioned above, this coordinate singularity does not define a classical horizon. To check this explicitly, it is useful to switch to Eddington-Finkelstein coordinates. Defining

the generalized tortoise coordinate as $dr_*^2 = G^{-1}F^{-1}dr^2$ and the advanced time as $v := t + r_*$, the metric (A1) can be expressed as

$$ds^2 = -G(r)dv^2 + 2F^{-1/2}(r)G^{1/2}(r)dvdr + r^2d\Omega^2. \tag{A6}$$

Notice that $2F^{-1/2}G^{1/2}dvdr = -(-ds^2 - Gdv^2 + r^2d\Omega^2)$. Therefore for causal ($ds^2 \leq 0$) and future-directed ($dv > 0$) curves, $dr < 0$ is only possible if $G(r) < 0$. If there were a critical point where $G(r) = 0$, it would define a one-way membrane for radial ($d\Omega = 0$) null geodesics, i.e. a horizon. But in our case $G(r) > 0$ for all $r \geq r_0$, so there is no horizon in this spacetime.

As a side remark, notice that in sharp contrast to the Schwarzschild metric where $F(r) = G(r)$, the Eddington-Finkelstein coordinates are not useful to penetrate across the coordinate singularity $r = r_0$, because the metric in these coordinates is not regular. We discuss the question of how to extend the metric across $r = r_0$ in Sec. IV.

[1] B. P. Abbott *et al.* (LIGO Scientific Collaboration and Virgo Collaboration) Phys. Rev. Lett. **116,** 061102 (2016).

[2] The Event Horizon Telescope Collaboration *et al.*, Astrophys. J. Lett. **875,** L1 (2019).

[3] V. Cardoso and P. Pani, Living Rev. Relativity **22,** 4 (2019).

[4] S. L. Shapiro and S. A. Teukolsky, *Black Holes, White Dwarfs, and Neutron Stars: The Physics of Compact Objects* (Wiley, New York, 1983).

[5] F. E. Schunck and E. W. Mielke, Classical Quantum Gravity **20,** R301 (2003).

[6] G. Raposo, P. Pani, M. Bezares, C. Palenzuela, and V. Cardoso, Phys. Rev. D **99,** 104072 (2019).

[7] P. O. Mazur and E. Mottola, Proc. Natl. Acad. Sci. U.S.A. **101,** 9545 (2004); Classical Quantum Gravity **32,** 215024 (2015).

[8] B. Holdom and J. Ren, Phys. Rev. D **95,** 084034 (2017).

[9] S. D. Mathur, Fortschr. Phys. **53,** 793 (2005).

[10] R. Brustein and A. J. M. Medved, Fortschr. Phys. **65,** 1600114 (2017).

[11] N. D. Birrel and P. C. W. Davies, *Quantum Fields in Curved Space* (Cambridge University Press, Cambridge, England, 1984).

[12] L. Parker and D. Toms, *Quantum Field Theory in Curved Spacetime* (Cambridge University Press, Cambridge, England, 2009).

[13] B-L. Hu and E. Verdaguer, *Semiclassical and Stochastic Gravity: Quantum Field Effects on Curved Spacetime* (Cambridge University Press, Cambridge, England, 2020).

[14] P. R. Anderson, W. A. Hiscock, and D. A. Samuel, Phys. Rev. D **51,** 4337 (1995).

[15] A. Levi and A. Ori, Phys. Rev. D **91,** 104028 (2015).

[16] A. Levi, E. Eilon, A. Ori, and M. van de Meent, Phys. Rev. Lett. **118,** 141102 (2017).

[17] A. Fabbri and J. Navarro-Salas, *Modeling Black Hole Evaporation* (ICP-World Scientific, London, England, 2005).

[18] A. Fabbri, S. Farese, J. Navarro-Salas, G. J. Olmo, and H. Sanchis-Alepuz, Phys. Rev. D **73,** 104023 (2006); J. Phys. Conf. Ser. **33,** 457 (2006).

[19] P. M. Ho and Y. Matsuo, Classical Quantum Gravity **35,** 065012 (2018).

[20] J. Arrechea, C. Barceló, R. Carballo-Rubio, and L. J. Garay, Phys. Rev. D **101,** 064059 (2020).

[21] R. Carballo-Rubio, Phys. Rev. Lett. **120,** 061102 (2018).

[22] P. M. Ho and Y. Matsuo, J. High Energy Phys. 03 (2018) 096.

[23] J. Arrechea, C. Barceló, R. Carballo-Rubio, and L. J. Garay, Phys. Rev. D **104,** 084071 (2021); Sci. Rep. **12,** 15958 (2022).

[24] P. M. Ho, H. Kawai, Y. Matsuo, and Y. Yokokura, J. High Energy Phys. 11 (2018) 056.

[25] J. L. Jaramillo, R. P. Macedo, and L. A. Sheikh, Phys. Rev. X **11,** 031003 (2021); Phys. Rev. Lett. **128,** 211102 (2022).

[26] V. Boyanov, K. Destounis, R. P. Macedo, V. Cardoso, and J. L. Jaramillo, Phys. Rev. D **107,** 064012 (2023).

[27] I. Agullo, V. Cardoso, A. del Rio, M. Maggiore, and J. Pullin, Phys. Rev. Lett. **126,** 041302 (2021); Int. J. Mod. Phys. D **30,** 2142013 (2021).

[28] S. Chakraborty, E. Maggio, A. Mazumdar, and P. Pani, Phys. Rev. D **106,** 024041 (2022); R. Dey, S. Chakraborty, and N. Afshordi, Phys. Rev. D **101,** 104014 (2020).

[29] B. Schutz, *A First Course in General Relativity* (Cambridge University Press, Cambridge, England, 2009).

[30] P. Candelas, Phys. Rev. D **21,** 2185 (1980).

[31] S. M. Christensen and S. A. Fulling, Phys. Rev. D **15,** 2088 (1977).

[32] R. M. Wald, Phys. Rev. D **17,** 1477 (1978).

[33] P. R. Anderson, R. Balbinot, and A. Fabbri, Phys. Rev. Lett. **94,** 061301 (2005).

[34] C. V. Vishveshwara, J. Math. Phys. (N.Y.) **9,** 1319 (1968).

[35] Matt Visser, *Lorentzian Wormholes: From Einstein to Hawking* (Washington University, St. Louis, 1995).

[36] F. S. N. Lobo, *Wormholes, Warp Drives and Energy Conditions* (Springer, Berlin, 2017), Vol. 189.

[37] G. Galloway, Ann. Henri Poincaré **1,** 543 (2000).

[38] V. Cardoso, E. Franzin, and P. Pani, Phys. Rev. Lett. **116,** 171101 (2016); **117,** 089902(E) (2016).

[39] G. Khanna and R. H. Price, Phys. Rev. D **95,** 081501 (2017).

[40] S. Iyer and C. M. Will, Phys. Rev. D **35,** 3621 (1987); S. Iyer, Phys. Rev. D **35,** 3632 (1987).

[41] E. Berti, V. Cardoso, and A. O. Starinets, Classical Quantum Gravity **26,** 163001 (2009).

[42] I. Agullo, A. del Rio, and J. Navarro-Salas, Phys. Rev. Lett. **118,** 111301 (2017); Phys. Rev. D **98,** 125001 (2018).

[43] J. Arrechea, C. Barcelo, R. Carballo-Rubio, and L. J. Garay, Phys. Rev. D **107,** 085005 (2023).